Int J Adv Manuf Technol (2018) 94:1335–1347
DOI 10.1007/s00170-017-0949-y

ORIGINAL ARTICLE

Modelling of surface roughness and grinding forces using artificial neural networks with assessment of the ability to data generalisation

D. Lipiński [1] · B. Bałasz [1] · Ł. Rypina [1]

Received: 18 April 2017 / Accepted: 10 August 2017 / Published online: 26 August 2017

Abstract The article presents a new methodology for modelling the influence of parameters and conditions of surface grinding process on the value of roughness and grinding forces. Grinding processes are characterised by numerous factors influencing results of the process with a complex mechanism of the cumulative effects of their interactions. Therefore, authors for the development of the model used an artificial neural network. The input parameters of the model, apart from the processing parameters, were the properties of the workpiece and features of the grinding wheel. In the selection process of the neural model structure, an evaluation criterion was proposed which included the character of the influence of processing parameters on the resultant values of the grinding process for the given pair workpiece–tool. A high ability to data generalisation by the developed neural model was demonstrated.

Keywords Grinding · Modelling · Roughness · Grinding forces · Neural networks

Nomenclature

a_e	depth of cut, (μm),
c	workpiece specific heat, ($J \cdot kg^{-1} \cdot K^{-1}$)
d_{ns}	grinding wheel mean grain dimensions, (FEPA designation),
E_m	workpiece Young's modulus, (GPa),
E_{nn}	neural network error function,
E_U	neural network error for learning data,
E_V	neural network error for validation data,
E_{Test}	neural network error for test data,
F_t'	tangential component of the specific grinding force, (N/mm),
F_n'	normal component of the normal grinding force, (N/mm),
$f^{(i)}(.)$	neuron activation function in i-th layer of a neural network,
H_m	workpiece hardness, (HRC),
H_n	grinding wheel hardness,
H_{ns}	grinding wheel abrasive material hardness $H_{ns,}$ (Mohs scale),
K	number of outputs of a neural network,
K_m	neural network penalty function,
M	number of neurons in the hidden layer of a neural network,
N	number of inputs of a neural network,
R_m	workpiece tensile strength, (MPa),
Sa	workpiece surface roughness average, (μm),
T	neural network targets,
V_{ns}	grinding wheel percentage pore contribution, (%),
v_c	grinding wheel peripheral speed, (m/s),
v_{ft}	table tangential speed, (m/min),
v_{fa}	axial table feed speed, (mm/stroke),
W	weights of a neural network,
X	neural network inputs,
X_m	workpiece material properties,
X_n	grinding wheel properties,
X_p	grinding parameters,
Y	neural network outputs,
α	workpiece thermal expansion, ($10^{-6} \cdot K^{-1}$),
λ	workpiece thermal conductivity, ($W \cdot m^{-1} \cdot K^{-1}$),

✉ D. Lipiński
dariusz.lipinski@tu.koszalin.pl

[1] Department of Mechanical Engineering, Koszalin University of Technology, Raclawicka 15-17, 75-620 Koszalin, Poland

1 Introduction

Grinding processes are one of the basic methods of finishing. This processing aims at obtaining the determined parameters of a processed surface and the shape and dimensions accuracy of processed elements. A significant parameter determining the geometric microstructure of ground surface is its roughness [1]. Roughness parameters influence i.a. corrosion resistance, the surface area of the contact zone between mating surfaces of machine parts and the fatigue life of the processed elements [2, 3]. Grinding forces constitute the variable used for monitoring the grinding process and indirectly for the evaluation of the phenomena occurring during the process [4, 5]. Two grinding force components are distinguished in grinding processes: tangential grinding force and normal grinding force. The values of individual components and their interactions enable determining the dominant character of the removal of processed material. Moreover, the values of force components enable determination of the changes on the grinding wheel active surface [6]. The increasing of the abrasive wear and the loading up of the grinding wheel active surface result in the increase of component grinding forces, increase of thermal interactions within the grinding zone as well as the increase of residual stress in the workpiece surface layer.

An appropriate selection of the grinding process parameters that ensures obtaining the expected roughness parameters of the processed surface has been the subject of numerous studies. An overview of studies on the issue indicates the use of both analytical modelling methods and soft computing methods. In the papers [7–9], the influence of machining parameters on the values of grinding forces, temperature, specific energy and surface quality of the grinding process was analysed. Models have been developed to predict the roughness of the machined surface and the grinding temperature using both analytical methods and neural networks.

Choi et al. [10] presented a generalised model enabling the prediction of roughness and burns of the surfaces occurring in the grinding process of cylindrical surfaces with aluminium oxide grinding wheels. Stępień [11] proposed a probabilistic model for the prediction of surface roughness in the grinding process. The model included the randomness of distribution of active grains on the grinding wheel active surface and its influence on the undeformed chip thickness and the processed surface formation was determined. In the study [12], a model determining the influence of the grinding process parameters on the values of component grinding forces including the forces resulting from the chip formation and friction in the contact zone with the workpiece was presented. Younis et al. [13] proposed a model of component grinding forces including three stages of interaction between the abrasive grain and the workpiece: rubbing, ploughing and cutting. However, the developed empirical models require a series of experimental tests in order to determine their coefficients.

The determination of the influence of parameters and conditions of processing on the values of component grinding forces and the roughness parameters of the processed surface is a difficult task due to the multitude of factors influencing their value and the complex mechanism of cumulative effects of their interactions [1, 4]. As a result of this, the developed analytical models are created with the range of assumptions enabling simplification of the modelling process. Artificial neural networks enable an efficient approach to modelling the influence of numerous factors with unknown cumulative effects of their interactions. Numerous attempts have been presented in the literature to model the influence of processing parameters and conditions on the resultant values of processing [14], although only a small portion of these studies concerned grinding processes.

The use of neural network models in grinding processes was focused primarily on the issues of processing parameter selection and monitoring of the processes. In the study [15], a multilayer neural network was used for the prediction of roughness of the processed surface. The obtained neural network models were characterised by high degree of fit to the experimental data for both low and high work speeds. Ammamou et al. [16] demonstrated that the use of a multilayer neural network for the prediction of values of specific component grinding forces provides better results obtained from the regression model, the power model and the genetic algorithms. The use of neural network models for monitoring of grinding processes applies primarily to the modelling of interactions between the processing variables and the values explaining the state of abrasive tool or parameters of the processed surface parameters. The validity of using artificial intelligent methods for the estimation of processed surface roughness [17, 18], tool wear [19–21] and precision of the shape and dimensions of processed elements [22] was demonstrated.

The present study developed a neural model for grinding process of surfaces determining the influence of processing parameters and the parameters characterising the pair workpiece–grinding wheel on the roughness of the processed surface and values of the component grinding forces. The model was developed based on experimental test results conducted for different pairs of workpiece–grinding wheel. For the selection of neural network, a new methodology was proposed based on the criterion including, apart from the value of mean squared error, the direction and influence of processing parameters on the resultant values of the grinding process for the given pair workpiece–grinding wheel. This enabled obtaining the neural model with good ability to data generalisation.

2 Grinding process assumptions

The result of the grinding process is the effect of interactions of the grinding wheel active surface and the surface of the

workpiece. The character and type of these interactions depends on, i.e. parameters of grinding X_p, properties of the processed material X_m and properties of the grinding wheel X_n:

$$X = [X_p, X_m, X_n] \tag{1}$$

In terms of kinematics, the course of grinding primarily depends on the parameters of the grinding process X_p and properties of the grinding wheel X_n. These parameters determine the conditions of contact between grinding wheel and workpiece. Among others, they influence [1, 4] the length of the contact zone between grinding wheel and workpiece, number of active grains, mean distance between active grains, mean and maximum chip cross section. The main parameters of surface grinding X_p include grinding wheel peripheral speed v_c, tangential table speed v_{ft}, axial table feed speed v_{fa} and depth of cut a_e.

$$X_p = [v_c, v_{ft}, v_{fa}, a_e] \tag{2}$$

The size and shape of abrasive grains, properties of the processed material X_m and the parameters of the cooling process and characters of the processing fluid influence working conditions of cutting edges and the wear processes of abrasive grains and tool [23]. Mechanical and physical properties of the processed material X_m have an effect on the phenomena occurring in the contact zone between abrasive grain and the processed material. They influence the chip formation process and the size and shape of ridges in the cutting zone of the single grain. Moreover, they influence the depth of thermal impact zone. The basic parameters characterising the mechanical and physical properties of the processed material X_m were assumed as follows: tensile strength R_m, Young's modulus E_m, hardness H_m, thermal expansion α, thermal conductivity λ and specific heat c.

$$X_m = [R_m, E_m, H_m, \alpha, \lambda, c] \tag{3}$$

Significant parameters influencing both the course and the result of the grinding process are the parameters linked to the type and structure of grinding wheel X_n. The size of abrasive grains influences the number of active grains per active area unit of grinding wheel. An important parameter determining the grinding wheel structure is the percentage contribution of abrasive grains and the related percentage contribution of pores. This parameter influences the topography of grinding wheel influencing the mean distance between abrasive grains. Moreover, high porosity of the grinding wheel facilitates the cooling process of the processing zone as well as the removal of chips from grinding wheel working zone. Therefore, the main parameters describing the structure and type of grinding wheel X_n in the developed neural model were assumed as follows: abrasive material hardness H_{ns} (Mohs scale), mean grain dimensions (FEPA designation) d_{ns}, grinding wheel hardness H_n and percentage pore contribution V_{ns}.

$$X_n = [H_{ns}, d_{ns}, H_n, V_{ns}] \tag{4}$$

The selection of the elements of the output signal results from the assumption to use the neural model, i.e. for the evaluation of the grinding process. The evaluation of the grinding process and thus obtained results is possible through the analysis of among others [1, 4, 23]: roughness of the processed surface and component grinding forces. Surface roughness constitutes one of the main parameters for the evaluation of the ground surface quality. Moreover, it is one of the main criteria for the determination of abrasive tool life. It influences the operating properties of the workpiece, including its tribological and fatigue properties. Along with the decrease of surface roughness, fatigue limit of the processed elements increases and the intensity of abrasive and fatigue wear decreases [24].

Among multiple parameters describing the 3D topography [25] of the processed surface, parameter *Sa* plays an important role, which is the equivalent to the *Ra* parameter determined for the profile:

$$Sa = \frac{1}{M_r N_r} \sum_{i=1}^{M_r-1} \sum_{j=1}^{N_r-1} |z(x_i, y_i)| \tag{5}$$

where

Sa	arithmetic means of surface roughness deviation from the mean surface
M_r, N_r	number of measurement points on the length and width of the surface, respectively
x, y, z	surface coordinates

Grinding forces constitute the indicator characterising grinding capability of processed materials and they enable the assessment of the wear degree of an abrasive tool. The value of grinding forces is linked to the energy transformed during processing. Moreover, the coefficient of component grinding forces is a significant indicator demonstrating the character of the phenomena occurring in the grinding zone:

$$\frac{F_t'}{F_n'} = \frac{2}{\pi} \cdot cos\beta + \mu \tag{6}$$

where

F_t'	tangential component of the specific grinding force
F_n'	normal component of the normal grinding force
β	abrasive grain rake angle
μ	friction coefficient between abrasive tool and the processed surface

Considering the above, the output signal Y of the developed neural model is defined as follows:

$$Y = \left[Sa, F_n', F_t' \right] \tag{7}$$

The assumed output parameters of the neural model enable the use of the developed model for the prediction of the roughness of the processed surface and for monitoring and evaluation of the grinding process based on the course of values of component grinding forces.

3 Artificial neural networks

The use of neural networks for modelling is based on their ability to generalise relationships occurring in the process despite the presence of noise in learning signals and in cases of the occurrence of redundant or correlated signals [26, 27]. Issues explaining the principles of operation of artificial neural networks and their applications for modelling were discussed in numerous overview studies [14, 26]. The structure most commonly used in the literature for process modelling is a feedforward multilayer network.

Figure 1 presents the structure of a two-layer feedforward network with N input signals, M neurons in the hidden layer and K neurons in the output layer. A single neuron of such network processes input signal following the relationship:

$$y = f(u) = f\left(\sum_{i=0}^{N} x_i \cdot w_i \right) \tag{8}$$

where

- $f(.)$ neuron activation function
- u product of the input signals and neuron weights
- n number of neuron inputs
- x_i i-th input signal
- w_i i-th neuron weight

A multilayer network consists of neurons logically arranged in layers. The hidden layer of a neural network is the intermediary layer for the processing of the input data. The structure of a multilayer network may contain any number of hidden layers; however, for practical uses rarely more than two layers are used. The output layer is responsible for the generation of output signal. The network presented in Fig. 1 is a feedforward one (signals flow in the direction from input to output) with full connections, i.e. each neuron of the preceding layer is connected to each neuron of the following layer.

Mathematical explanation of i-th output y_i of the above network is as follows:

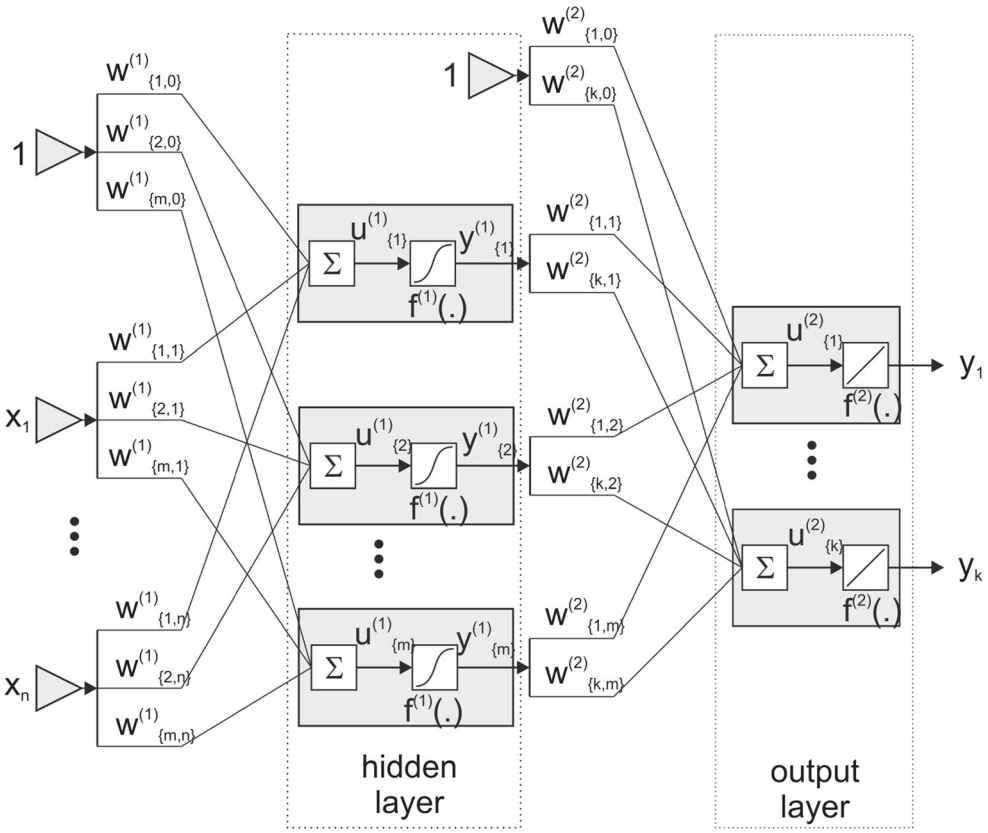

Fig. 1 Multilayer network structure

$$y_i = f^{(2)}\left[\sum_{j=0}^{m} w^{(2)}_{\{i,j\}} \cdot f^{(1)}\left(\sum_{k=0}^{n} w^{(1)}_{\{j,k\}} \cdot x_k\right)\right] \quad (9)$$

where

$f^{(i)}(.)$	neuron activation function in i-th layer
m	number of neurons in the hidden layer
n	number of network inputs
$w^{(i)}\{j,k\}$	weight connecting the j-th neuron from i-th layer with k-th neuron of the preceding layer
x_i	i-th network input signal

Multilayer neural network learning, understood as a modification of the weights W of network is conducted in the supervised learning mode. In the process, knowledge of both input signals X in the network and their target T signals is necessary.

Selection of weight W of a neural model is conducted in the manner ensuring minimization of the error function E, understood as:

$$E = \frac{1}{n}\sum_{i=1}^{n}(\mathrm{net}(X_i, W) - T_i)^2 \quad (10)$$

where

n	number of signals in the learning set
net	neural model
X_i	i-th input signal
W	neural model weights
T_i	target signal for i-th input signal

The neural model learning process assumes the presentation of neural network of subsequent examples of input signal X_i followed by such modification of the parameters of model W for the response of model Y = net(X_i,W) to be the most similar to the target signal T_i.

4 Methodology of neural model validation

The validation of neuron models learned in supervised mode assumes a validation based on dependence (7). This dependence verifies only the degree of consistency of the model's response with the data obtained from the experiment. The process of creating a neural model does not assume the selection of modelling function. Thus, the verification of a neural model based solely on the dependence (7) does not provide an answer to the correctness of the modelled relationship between the points of the experiment. This issue is of particular importance if the developed models are to be used to monitor, optimise or supervise grinding processes. In this case, evaluating the correctness of data interpolation becomes a key issue.

On the basis of experimental data, it is possible to assess the direction and magnitude of the influence of the parameters and conditions of machining X_p on the output variables of the grinding process Y for a given workpiece–grinding wheel pair. By determining the direction of the neural model response gradient, it is possible to evaluate the correctness of model interpolation.

Figure 2 shows a diagram of the neural model interpolation accuracy. For the specified setting parameter of the process $x_i \in X_p$, the values of gradient ΔY_{x_i} for i..P are determined. The value of function K_m is then determined according to the following relationship:

$$K_m = \frac{numel(\Delta Y \le 0)}{numel(\Delta Y)} \quad (11)$$

where

$\Delta Y = [\Delta Y_{x_1}, \Delta Y_{x_2}, \ldots, \Delta Y_{x_i}]$	gradient of the modelled relationship for the process parameters $x_i \in X_p$ of a given pair workpiece–grinding wheel
numel(.)	number of elements in the data set

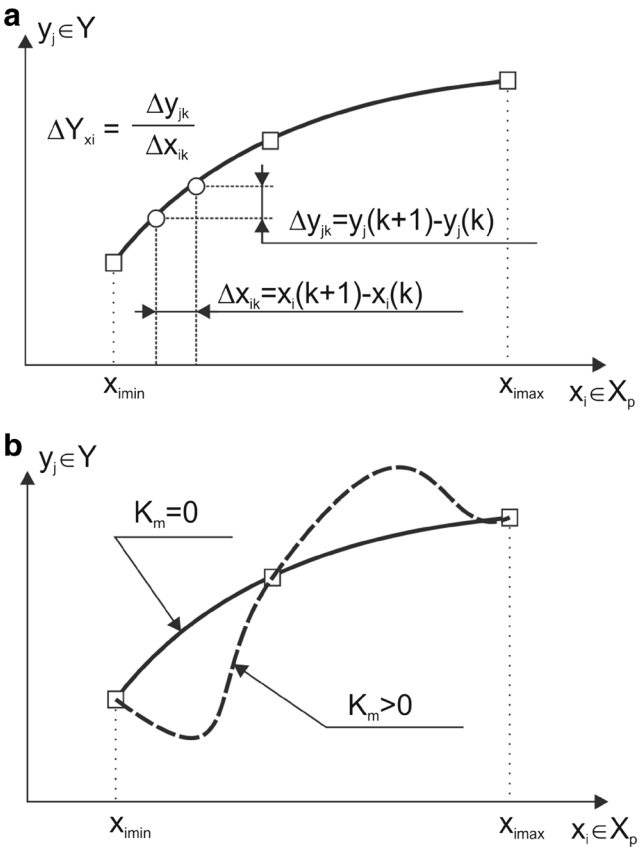

Fig. 2 The neural model interpolation accuracy, **a** Gradient determination, **b** Example of the course of modelled relationship for different K_m values

Table 1 Grinding parameters and conditions

	Materials		
	100Cr6	Ti-6Al-4V	Inconel 718
Grinding wheel	Grinding wheel A Grinding wheel C	Grinding wheel A Grinding wheel B	Grinding wheel A
Grinding wheel peripheral speed v_c	30 m/s	30 m/s	30 m/s
Tangential table speed v_{ft}	5 m/min 15 m/min 25 m/min	25 m/min	2 m/min 3 m/min 4 m/min
Axial table feed speed v_{fa}	3 mm/stroke	–	1 mm/stroke 2 mm/stroke 4 mm/stroke
Depth of cut a_e	5, 10, 20 μm	5, 10, 20 μm	5, 10, 20 μm

The above relationship assumes non-zero values for cases where the behaviour of the modelled dependence is nonincreasing. By changing the sign of inequality in the numerator, it is possible to analyse the different influence mature of the input parameters of the model.

The following relationship was used to validate the neural model:

$$E_{nn} = \mathrm{mse}(E_T) + K_m \tag{12}$$

where

$\mathrm{mse}(E_T)$ mean square error of the model response for test data

K_m penalty function (following Eq. 8)

5 Experimental study

The surface grinding process was examined. Peripheral grinding was performed with the process parameters and conditions described in Table 1. Samples used in experimental studies were made of: bearing steel 100Cr6, titanium alloy Ti-6Al-4V, Inconel® alloy 718. Parameters of the processed materials describing its physical and mechanical properties are listed in Table 2.

Table 2 Mechanical and physical properties of materials

	Materials		
	100Cr6	Ti-6Al-4 V	Inconel 718
Tensile strength R_m, MPa	720	880	1100
Young's modulus E_m, GPa	210	114	200
Hardness H_m, HRC	65	33	34
Thermal expansion α, $10^{-6} \cdot \mathrm{K}^{-1}$	10	9.7	13
Thermal conductivity λ, $\mathrm{W} \cdot \mathrm{m}^{-1} \cdot \mathrm{K}^{-1}$	25	7.1	11.2
Specific heat c, $\mathrm{J} \cdot \mathrm{kg}^{-1} \cdot \mathrm{K}^{-1}$	460	553	435

The measurement of the grinding force components was done using a piezoelectric dynamometer 9257B and a multichannel amplifier 5070A12100 by Kistler. The measurement data was registered at 10 kHz frequency using a 16-bit measurement card 2855A4 by Kistler.

Material was ground with aluminium oxide grinding wheels with different hardness. All used grinding wheels had the same dimensions, i.e. external diameter D = 250 mm and grinding wheel height H = 25 mm. The properties of grinding wheels and abrasive materials are presented in Table 3.

Parameters of the dressing operation of the grinding wheel active surface and parameters and conditions of cooling process were constant during all tests. The grinding parameters were selected to ensure the appropriate quality of the ground surfaces without the signs of chatter and burns. For the range of processing parameters presented in Table 1, a full factorial experiment was performed.

In order to determine repeatability of the obtained results, the tests were conducted three times. After the grinding process had been accomplished, processed surface roughness was analysed. A Talysurf CCI 6000 profilometer by Taylor Hobson was used for the measurement of surface topography. Twenty times magnification lens were used to enable the measurement of a surface with dimensions 0.9 mm × 0.9 mm. To

Table 3 Properties of used grinding wheels and abrasive materials

	Grinding wheel no.		
	A	B	C
Grinding wheel hardness H_n	K	M	P
Abrasive material hardness H_{ns}	9 (Mohs scale)		
Mean grain size d_z	120 μm		
Pore volume V_n	40.5%	37.5%	33.5%

record the data, a CCD sensor with resolution 1024 × 1024 points was used enabling the measurement of the processed surface with the horizontal resolution of 0.88 μm. Vertical resolution of the profilometer is up to 10 pm. For each of the samples, measurement was conducted three times in random places. The measurement results of each of the analysed samples were averaged.

6 Modelling assumptions

6.1 Structure of learning, verifying and test data

A set of input data of the neural model was developed based on the conducted experiments:

$$X = \left[a_e, v_{fa}, v_{ft}, H_n, V_n, R_m, E_m, H_m, \alpha, \lambda, \mathrm{c}\right] \tag{13}$$

and their target values:

$$T = \left[Sa, F_n^{'}, F_t^{'}\right] \tag{14}$$

The set of data used for neural network learning was divided into three subsets:

- Learning data subset U—enabling mapping of the modelled relationship—used at the network learning stage;
- Verifying data subset V—a subset separated from the learning data; prevents the phenomenon of excessive matching of network responses to data included in the learning subset—used at the network learning stage;
- Test data subset Test—subset of data determining the quality of modelled relationship, and not used at the network learning stage; ability to map the test data set by the network is the measure of the ability to generalise the modelled relationship.

Data obtained from the experiment were divided into the above subsets in 70:15:15 ratio for each workpiece–grinding wheel pair.

6.2 Selection of the neural model structure

For artificial neural networks being used for process modelling, determination of the proper network architecture is a significant issue. The problem of neural network architecture optimisation is complex due to the multitude of factors influencing the result of modelling, which includes:

- A large number of neural network structures, resulting from the direction of the weight connections, number of neurons in the hidden layer as well as the used functions of neuron activation
- Large set of neural network learning algorithms
- Random selection of the initial values of weights in a neural network, thus random starting point of optimisation of the weight modification algorithm

The results of numerous studies demonstrate that a single-layer feedforward network constitutes the most commonly used network type. In reference to this structure, numerous studies and mathematical proofs have been conducted [28, 29] indicating the fact that a multilayer network is a universal approximator of complex nonlinear functions.

For the modelling of relationships occurring in the grinding process, a multilayer network with sigmoidal functions of activation in the hidden layers and linear functions of activation in the output layer was used. For the search of an optimised architecture of the neural model, the following procedure was implemented:

Stage 1. The creation of neural models with one and two hidden layers. The maximum number of neurons in the first hidden layer was established as $N = 50$, and in the second hidden layer $M = 20$. Networks with a given architecture were created for $K = 20$ times for each of them generating the initial weight values at random. As a result, $N \times K$ of two-layer networks and $N \times M \times K$ of three-layer networks were obtained.
Stage 2. Estimation of the modelling error value E_{nn} for the created neural networks. Experimental data used for the creation of the models indicate a monotonous (increasing) character of the modelled relationships for each of the pairs of workpiece–grinding wheel. The use of penalty function K_m enables determination whether the developed models of relationships between the influences of processing parameters on the results of the process reflect the influence character. Thus, the modelling error was determined using the relationship (9).
Stage 3. Selection of the neural model minimising the error value E_{nn}.

6.3 Neural network learning method

The supervised learning method with the backpropagation algorithm was used in the created neural models. Weight matrices were modified following the Lavenberg-Marquardt algorithm:

$$\Delta W(t) = -(H + \eta I)^{-1}\left(\frac{\delta E(W(t-1))}{\delta W}\right) \tag{15}$$

where

W weight matrix

Table 4 Value of modelling errors for 10 two-layer structures with the lowest modelling error value E_{nn}

Structure	Mean square error for			K_m	E_{nn}
	Learning data E_U	Verifying data E_V	Test data E_{Test}		
11-4-3	0.0409	0.0404	0.0858	0.0176	0.1034
11-4-3	0.0443	0.0427	0.0658	0.0704	0.1362
11-6-3	0.0394	0.0351	0.0672	0.0768	0.1440
11-5-3	0.0415	0.0416	0.0722	0.1664	0.2386
11-5-3	0.0439	0.0430	0.0644	0.1944	0.2588
11-8-3	0.0333	0.0351	0.0728	0.1912	0.2640
11-11-3	0.0369	0.0374	0.0813	0.1880	0.2693
11-5-3	0.0410	0.0389	0.0955	0.1888	0.2843
11-14-3	0.0285	0.0368	0.0705	0.2168	0.2873
11-5-3	0.1137	0.0732	0.1502	0.1752	0.3254

H objective function hessian
η Marquardt's coefficient
I identity matrix
t learning step

Adaptive value of coefficient η was used. Initial value of the coefficient was set at 0.001, the increase coefficient to the value 10 and reduction coefficient to value 0.1. In the case, when as a result of weight modification in the subsequent learning step the value of the error E is reduced, the value of the coefficient η is also reduced. Close to minimum of error function the algorithm behaves like a gradient algorithm, whereas at a large distance from the minimum like the steepest descent algorithm. This results in a considerable increase of the convergence of the neural network learning process.

7 Analysis of the results

7.1 Analysis of the results of neural network structure selection

Results of modelling using two-layer networks presented in Table 4 indicate that the best results were obtained for the 11-4-3 network containing four neurons in the hidden layer. Values of the error E_{nn} were the lowest for this network. Increase of the number of neurons in the hidden layer leads to the decrease of the mean square error value for learning data together with the increase of this value for test data. This indicates the occurrence of neural network overfitting; thus, a loss of the ability to generalise relationships included in the experimental data.

Penalty function K_m for the developed two-layer neural models takes a non-zero value. It indicates that not all modelled relationships properly reflect character of grinding parameters influence on output values. The observed non-zero value of the penalty function K_m for the two-layer model may stem from the occurrence of discontinuity between the values of the modelled data for individual pairs of workpiece–grinding wheel. An improvement of the ability to model discontinuous relationships requires the use of an additional hidden layer.

Results of modelling with the use of three-layer networks presented in Table 5 demonstrate the validity of mapping of the monotonous relationships for individual pairs of workpiece–grinding wheel. In the case of each neural model included in Table 5, the penalty function K_m takes the value of zero. Among the created and learned 20,000 three-layer neural networks, the lowest value of the modelling error E_{nn} was obtained for the network with the structure 11-8-9-3 containing 17 neurons distributed in two hidden layers. The sum of the mean square error of the mapping of the experimental data determined based on the test set mse(E_{Test}) and the penalty function K_m assumes the lowest value for this network.

Table 5 Value of modelling errors for 10 three-layer structures with the lowest modelling error value E_{nn}

Structure	Mean square error for			K_m	E_{nn}
	Learning data E_U	Verifying data E_V	Test data E_{Test}		
11-8-9-3	0.0395	0.0464	0.0792	0	0.0792
11-3-4-3	0.0456	0.0525	0.0795	0	0.0795
11-3-10-3	0.0574	0.0560	0.1177	0	0.1177
11-2-4-3	0.0572	0.0603	0.1199	0	0.1199
11-2-3-3	0.0882	0.0682	0.1251	0	0.1251
11-2-3-3	0.1212	0.0836	0.1316	0	0.1316
11-2-2-3	0.1070	0.0779	0.1624	0	0.1624
11-2-2-3	0.1606	0.0861	0.2225	0	0.2225
11-1-2-3	0.2271	0.0963	0.2593	0	0.2593
11-1-1-3	0.2489	0.0982	0.2708	0	0.2708

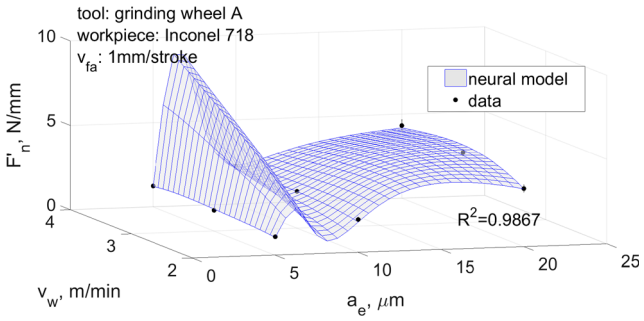

Fig. 3 An example of an erroneously developed neural model determining the relationship between processing parameters with the values of the specific normal grinding force; workpiece: Inconel 718, tool: grinding wheel A, v_{fa} = 1 mm/stroke

The lowest mean value of modelling error mse(E_{Test}) = 0.0309 among all created networks was obtained for the structure 11-2-19-3. However, in its case the value of the penalty function K_m assumed the value of 0.72, which indicated low ability of the model for a correct interpolation of the relationships included in the experimental data (Fig. 3).

The model correctness cannot be holistically evaluated using only the error value determined from experimental data E_{Test}. The error value E_{Test} indicates solely the correctness of mapping of the relationships in the experimental points. It does not provide information on the character of the relationships between individual points of the experiment. Introduction of the penalty function K_m enables the evaluation of the correctness of interpolations of the developed neural models.

7.2 Verification of neural model correctness

The accuracy of mapping the experimental data by the neural model with structure 11-8-9-3 was determined. The analysis of the linear regression results between the response value *Y* of the model and the target value *T* was conducted. In the assumption of the above analysis for the full mapping of data, the relationship $Y = T$ should be fulfilled, and value of the linear regression coefficient *R* should be 1.

Figure 4 presents the high ability to represent the test data by the developed neural model. The lowest value of fitting of the neural model response was observed for the value of processed surface roughness parameter *Sa* (R = 0.95). The lower ability of mapping processed surface roughness parameter *Sa* by the neural model is influenced by the fact that its values, apart from the values included as the inputs in the developed model, are influenced by the values related to the changes on the grinding wheel active surface. The main reason for the changes on the grinding wheel active surface is the wear processes (abrasive and fracture wear) and the loading up of the grinding wheel active surface. Influence of these factors on the value of surface roughness parameters is not included in the developed neural model, and the character of these interactions can only be indirectly determined in the model through the relationship between the assumed processing parameters and conditions and changes on the grinding wheel active surface.

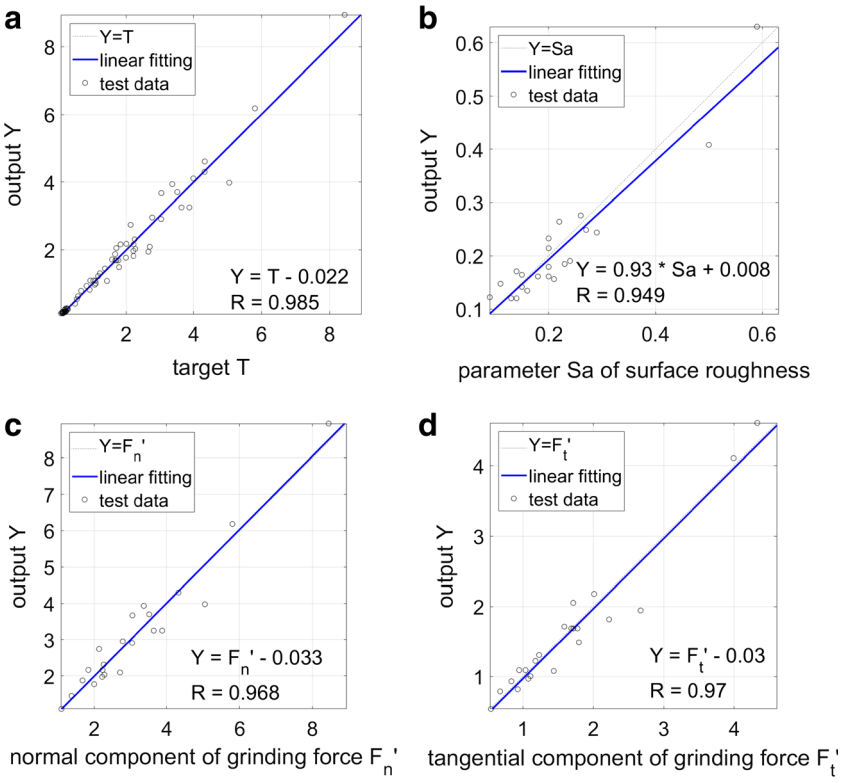

Fig. 4 Analysis of the mapping level of the test data set by the neural model for **a** all modelled output values (Sa, F_n', F_t'), **b** surface roughness parameter *Sa*, **c** specific normal component F_n', and **d** specific tangential component F_t' of grinding force

Table 6 List of values of the determination factor R^2 for the partial models explaining the influence of processing parameters on the output values of the model for individual pairs of workpiece–grinding wheel

Lp	Processed material	Grinding wheel	v_{fa}, mm/stroke	Partial model	R^2
1	Inconel 718	A	4	Sa = f(a_e, vw)	0.9254
2	Inconel 718	A	4	F_n' = f(a_e, vw)	0.9885
3	Inconel 718	A	4	F_t' = f(a_e, vw)	0.9832
4	Inconel 718	A	2	Sa = f(a_e, vw)	0.8686
5	Inconel 718	A	2	F_n' = f(a_e, vw)	0.9132
6	Inconel 718	A	2	F_t' = f(a_e, vw)	0.9346
7	Inconel 718	A	1	Sa = f(a_e, vw)	0.8150
8	Inconel 718	A	1	F_n' = f(a_e, vw)	0.9380
9	Inconel 718	A	1	F_t' = f(a_e, vw)	0.9502
10	Ti6Al4V	A	13	Sa = f(a_e, 25)	0.8155
11	Ti6Al4V	A	13	F_n' = f(a_e, 25)	0.9988
12	Ti6Al4V	A	13	F_t' = f(a_e, 25)	0.9999
13	Ti6Al4V	B	13	Sa = f(a_e, 25)	0.9938
14	Ti6Al4V	B	13	F_n' = f(a_e, 25)	0.9949
15	Ti6Al4V	B	13	F_t' = f(a_e, 25)	0.9956
16	100Cr6	A	3	Sa = f(a_e, vw)	0.9486
17	100Cr6	A	3	F_n' = f(a_e, vw)	0.9913
18	100Cr6	A	3	F_t' = f(a_e, vw)	0.9719
19	100Cr6	C	3	Sa = f(a_e, vw)	0.7557
20	100Cr6	C	3	F_n' = f(a_e, vw)	0.9675
21	100Cr6	C	3	F_t' = f(a_e, vw)	0.9653

Consistence in terms of the values of response of the neural model Y with the target values determined as a result of the experiment generally explains the correctness of the neural model. A detailed analysis requires the evaluation of the partial models explaining the influence of processing parameters on the surface roughness parameter Sa and values of the specific component grinding forces F_n' and F_t' on the individual pairs of workpiece–grinding wheel. To this end, for individual partial models included in Table 6, the values of the determination factor R^2 were calculated. Factor R^2 indicates which part of the variation of the output values was explained by the developed neural model.

The mean value of the determination factor R^2 for the partial models included in the Table 6 is 0.94. This indicates the fact that a significant part of variations of the output values of the neural model (surface roughness parameter Sa, specific normal component grinding force F_n' and specific component tangential grinding force F_t') stem from its dependency on the processing parameters assumed in the model.

The lowest values of the determination factor R^2 were obtained for the partial models explaining the influence of the process parameters on the value of surface roughness parameter Sa. The value of this factor for the pair: Inconel 718–grinding wheel A is 0.82, and for the pair: bearing steel 100Cr6–grinding wheel C is 0.76. A graphic demonstration of example results of modelling the influence of the process parameters on the value of surface roughness Sa parameter is presented in Fig. 5.

Precision of modelling the influence of process parameters and conditions on the value of surface roughness parameter Sa is variable. For different pairs of workpiece–grinding wheel,

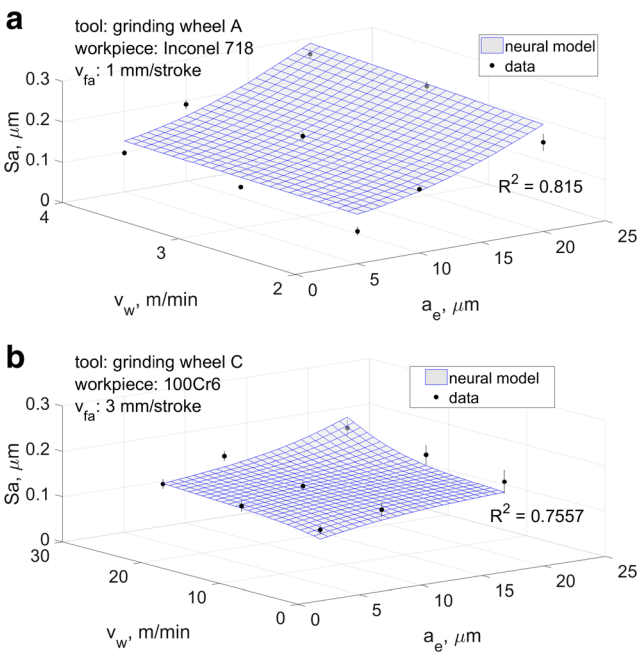

Fig. 5 Neural model determining the relationship between the processing parameters with values of the surface roughness parameter Sa for the pair **a** Inconel 718–grinding wheel A and **b** bearing steel 100Cr6–grinding wheel C

the quality of the partial model determined with the value of factor R^2 assumes values from 0.7557 to 0.9956. The formation of the grinding wheel active surface has a significant influence on the result of the grinding process determined as the roughness of the processed surface. As a result of this process, geometric properties of the grinding wheel active surface are shaped, which depend on both its formation process and on the properties of the grinding wheel. Moreover, as a result of the interaction of the grinding wheel active surface with the workpiece, changes in their condition take place. The degree and rate of these changes depend on the properties of the workpiece and the grinding wheel, and, indirectly, on the process parameters and conditions. The degree of influence of these factors and the mechanism of accumulation of the results of their interactions may differ for different pairs of workpiece–grinding wheel. As a consequence, a high variability of the level of fitting of individual partial models occurs.

The modelling precision is further influenced by the need to map the discontinuities in the modelled relationships. Such discontinuity occurs between the values of the output value of the model for individual pairs of workpiece–grinding wheel. Modelling precision could be enhanced via increasing the number of neurons in the hidden layers of the neural network. However, as it has been demonstrated by the previous analysis, this results in a decrease of the ability to data generalisation by the neural model.

The highest modelling precision was obtained for the partial models determining the influence of process parameters and conditions on the value of the specific component of grinding forces. Example results of modelling are presented in Figs. 6 and 7.

Value of the determination factor R^2 of the partial models explaining the influence of the parameters and conditions of processing on the specific component grinding force remains in the range from 0.91 to 0.99. The set of input values included in the model to a large degree describes (mean in approx. 97%) the variation of values of both component of grinding forces.

The use of three-layer network for modelling the influence of process parameters and conditions on the value of surface

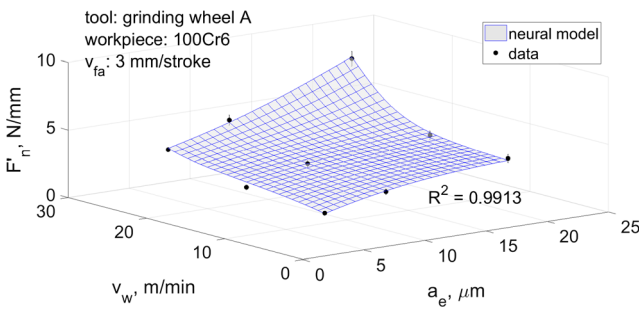

Fig. 6 Neural model determining the relationship between the processing parameters and the values of the specific normal component of grinding force, workpiece: bearing steel 100Cr6, tool: grinding wheel A

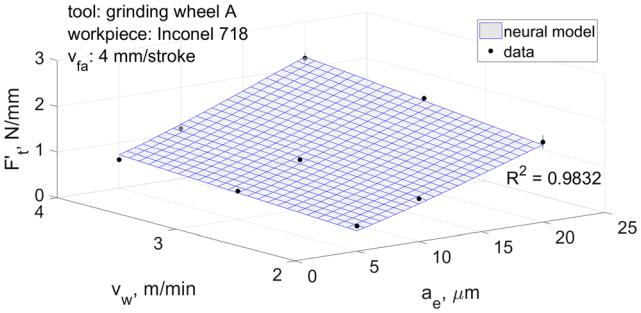

Fig. 7 Neural model determining the relationship between the processing parameters and the values of the specific tangential component of grinding force, workpiece: Inconel alloy 718, tool: grinding wheel A

roughness parameter Sa and component of grinding forces of three-layer networks enables obtaining of a model with high fitting degree to the experimental data. The mean value of the determination factor R^2 determined for the partial models listed in Table 6 is 0.94.

Value of the penalty function K_m for the three-layer network model assumes zero value. The use of the penalty function K_m for the evaluation of the modelling correctness results in the developed partial models with getting the form of a continuous function with values increasing with the increase of the processing parameter values. This corresponds to the character of the relationships included in the experimental data.

8 Conclusion

The article presents a methodology for the creation of neural models for surface grinding process. As a result of the conducted experimental study, data sets were developed enabling the conduct of the neural network learning allowing modelling the influence of processing parameters and conditions on the values of the specific component grinding forces F_n' and F_t' and the parameter Sa of surface roughness. As a result of the conducted tests and analyses on modelling of the abrasive processing using multilayer networks, it can be stated that:

- Evaluation of the correctness of neural network modelling solely on the basis of value of the error determined for the test data set does not allow for the full evaluation of the correctness of mapping of the relationships occurring in the experimental data set.
- The proposed penalty function K_m determining the correctness of data interpolations enables the selection of a model from the set of neural models with a high ability to data generalisation.
- The neural models created using three-layer networks are characterised by a high degree of mapping of the

relationships occurring in the experimental data (penalty function $K_m = 0$, mean regression coefficient $R^2 = 0.985$).
- A detailed analysis of the developed neural model indicates its higher ability for predicting the specific grinding forces F_n', F_t' then surface roughness parameter Sa. This is linked with the large number of factors influencing the roughness parameters and the complexity of the accumulation mechanism of their results.

The developed neural models enable the prediction of processed surface roughness parameter Sa and values of the component grinding forces F_n' and F_t'. This enables both optimisation of the processing parameters in order to obtain established surface roughness values and the use of the neural model for monitoring of grinding processes.

Acknowledgements The authors would like to thank Joanna Wieczyńska, MSc from the International Cooperation Office of Koszalin University of Technology for manuscript proofreading.

Funding This study was funded by National Science Centre, Poland (grant # NN 503 557940).

Compliance with ethical standards

Conflict of interest The authors declare that they have no conflict of interest.

References

1. Shaw M (1996) Principles of abrasive processing. Oxford University Press, New York
2. Majidi AP, Streicher MA (1984) The effect of methods of cutting and grinding on sensitisation in surface layers on AISI 304 stainless steel. Corrosion 40:445–458. doi:https://doi.org/10.5006/1.3577915
3. Rhouma AB, Sidhom H, Braham C (2001) Effects of surface preparation on pitting resistance, residual stress and stress corrosion cracking in austenitic stainless steels. J Mater Eng Perform 10:507–514. doi:https://doi.org/10.1361/105994901770344638
4. Malkin S (1989) Grinding technology. Theory and applications of machining with abrasives. Ellis Horwood, New York
5. Ding WF, Xu JH, Chen ZZ, Yang CY, Song CJ, Fu YC (2013) Fabrication and performance of porous metal-bonded CBN grinding wheels using alumina bubble particles as pore-forming agents. Int J Adv Manuf Technol 67:1309–1315. doi:https://doi.org/10.1007/s00170-012-4567-4
6. Li ZC, Lin B, Xu YS, Hu J (2002) Experimental studies on grinding forces and force ratio of unsteady-state grinding technique. J Mater Process Technol 129:76–80. doi:https://doi.org/10.1016/S0924-0136(02)00579-4
7. Xi X, Ding W, Li Z, Xu J (2017) High speed grinding of particulate reinforced titanium matrix composites using a monolayer brazed cubic boron nitride wheel. Int J Adv Manuf Technol 90:1529–1538. https://doi.org/10.1007/s00170-016-9493-4
8. Li Z, Ding W, Liu C, Su H (2017) Prediction of grinding temperature of PTMCs based on the varied coefficients of friction in conventional-speed and high-speed surface grinding. Int J Adv Manuf Technol 90:2335–2344. doi:https://doi.org/10.1007/s00170-016-9578-0
9. Liu C, Ding W, Li Z, Yang C (2017) Prediction of high-speed grinding temperature of titanium matrix composites using BP neural network based on PSO algorithm. Int J Adv Manuf Technol 89:2277–2285. doi:https://doi.org/10.1007/s00170-016-9267-z
10. Choi TJ, Subrahmanya N, Li H, Shin YC (2008) Generalized practical models of cylindrical plunge grinding processes. Int J Mach Tools Manuf 48:61–72. doi:https://doi.org/10.1016/j.ijmachtools.2007.07.010
11. Stępień P (2008) A probabilistic model of the grinding process. Appl Math Model 33:3863–3884. doi:https://doi.org/10.1016/j.apm.2009.01.005
12. Malkin S, Cook NH (1971) The wear of grinding wheels: part 1—attritious wear. J Eng Ind 93:1120–1128. doi:https://doi.org/10.1115/1.3428051
13. Younis M, Sadek MM, El-Wardani T (1987) A new approach to development of a grinding force model. J Eng Ind 109:306–313. doi:https://doi.org/10.1115/1.3187133
14. Pontes FJ, Ferreira JR, Silva MB, Paiva AP, Balestrassi PP (2010) Artificial neural networks for machining processes surface roughness modeling. Int J Adv Manuf Technol 49:879–902. doi:https://doi.org/10.1007/s00170-009-2456-2
15. Nabil BF, Amamou R (2006) Ground surface roughness prediction based upon experimental design and neural network models. Int J Adv Manuf Technol 31:24–36. doi:https://doi.org/10.1007/s00170-005-0169-8
16. Amamou R, Nabil BF, Farhat F (2008) Improved method for grinding force prediction based on neural network. Int J Adv Manuf Technol 39:656–668. doi:https://doi.org/10.1007/s00170-007-1264-9
17. Aquiar PR, Cruz CED, Paula WCF, Bianchi EC, Thomazella R, Dotto FRL (2007) Neural network approach for surface roughness prediction in surface grinding. Proceedings of the 25th IASTED International Multi-Conference: Artificial Intelligence and Applications, pp 96–101
18. Chang CH, Tsai JC, Chiu NH, Chein RY (2010) Modeling surface roughness and hardness of grinding SKD11 steel using adaptive network based fuzzy inference. Adv Mater Res 126-128:171–176. doi:https://doi.org/10.4028/www.scientific.net/AMR.126-128.171
19. Nakai ME, Junior HG, Aguiar PR, Bianchi EC, Spatti DH (2015) Neural tool condition estimation in the grinding of advanced ceramics. IEEE Lat Am Trans 13:62–68. doi:https://doi.org/10.1109/TLA.2015.7040629
20. Moia DFG, Thomazella IH, Aguiar PR, Bianchi EC, Martins CHR, Marchi M (2015) Tool condition monitoring of aluminum oxide grinding wheel in dressing operation using acoustic emission and neural networks. J Braz Soc Mech Sci Eng 37:627–640. doi:https://doi.org/10.1007/s40430-014-0191-6
21. Lezański P (2001) An intelligent system for grinding wheel condition monitoring. J Mater Process Technol 109:258–263. doi:https://doi.org/10.1016/S0924-0136(00)00808-6
22. Lipiński D, Kacalak W (2007) Assessment of the accuracy of the process of ceramics grinding with the use of fuzzy interference. Adaptive and Natural Computing Algorithms ICANNGA. Lecture Notes in Computer Science, vol 4431. pp 596–603. doi:https://doi.org/10.1007/978-3-540-71618-1_66
23. Oczoś KE, Porzycki J (1986) Grinding—the basis and technique. WNT, Warsaw

24. Grzesik W (2015) Effect of the machine parts surface topography features on the machine service. Mechanik 8–9:587–593. doi: https://doi.org/10.17814/mechanik.2015.8-9.493
25. ISO 25178–2:2012 Geometric product specifications (GPS)—surface texture: areal—part 2: terms, definitions and surface texture parameters, International Organization for Standardization
26. Chandrasekaran M, Muralidhar M, Murali Krishna C, Dixit US (2010) Application of soft computing techniques in machining performance prediction and optimization: a literature review. Int J Adv Manuf Technol 46:445–464. doi:https://doi.org/10.1007/s00170-009-2104-x
27. Lipiński D, Ratajski J (2007) Modeling of microhardness profile in nitriding processes using artificial neural network. International Conference on Intelligent Computing ICIC 2007: Advanced Intelligent Computing Theories and Applications. Lecture Notes in Computer Science, vol 4682. pp 245–252. doi:https://doi.org/10.1007/978-3-540-74205-0_27
28. Hornik K, Stinchcombe M, White H (1989) Multilayer feedforward networks are universal approximators. Neural Netw 2:359–266. doi:https://doi.org/10.1016/0893-6080(89)90020-8
29. Hornik K (1991) Approximation capabilities of multilayer feedforward networks. Neural Netw 4:251–257. doi:https://doi.org/10.1016/0893-6080(91)90009-T